Kinetics and Mechanisms of Nucleophilic Displacements with Heterocycles as Leaving Groups. Part 25.[1] *X*-Ray Structure Determinations, Crystallographic Evidence for Steric Crowding, and Correlation with Acceleration of Rates

Alan R. Katritzky *
Department of Chemistry, University of Florida, Gainesville, Florida 32611, U.S.A.
Doriano Lamba and Riccardo Spagna
Istituto di Strutturistica Chimica, Giordano Giacomello, Casella Postale N.10, 00016 Monterotondo Stazione, Roma, Italy
Alessandro Vaciago
Chemical Crystallography Laboratory, University of Oxford, Oxford OX1 3PD
Roland Prewo and Jost H. Bieri
Organisch-Chemisches Institut, Universitat Zurich, CH-8057 Zurich, Switzerland
John J. Stezowski
Institut für Organische Chemie, Biochemie und Isotopenforschung Universitat Stuttgart, D-7000 Stuttgart 80, Federal Republic of Germany
Giuseppe Musumarra
Dipartimento di Scienze Chimiche, Universita di Catania, Viale A. Doria 6, 95125 Catania, Italy

X-Ray crystallographic structures are determined for seven *N*-benzylpyridinium salts including compounds possessing free, five-ring fused, and six-ring fused α-phenyl groups. Significant bond lengths, non-bonding distances, torsional and interplanar angles are determined and compared for the eight structures (the triphenyl derivative was found in two crystal environments). The results show steric overcrowding to an extent that parallels the kinetic displacement rates. However, the steric strain existing in all these molecules is relieved to different extents by different distortions in the different molecules. Nevertheless, crystallographic interatomic distances and angles are shown to be of potential utility in determining the type of mechanistic changes to be undergone, provided the appropriate parameters are selected.

Previous Parts have discussed in detail the effect of the leaving group on the kinetic rates of nucleophilic displacements of nitrogen substituents from substituted pyridinium cations.[2] It was found that the structure of the leaving group could strongly influence the rates which extended over five orders of magnitude for *N*-benzyl compounds.[3,4] These rate differences were rationalized in terms of steric acceleration by bulky α-substituents, resulting from increased strain in the ground states of these substrates. Thus, for example, in the series, (**1**), (**3**), and (**7**), the rates for reaction with piperidine in chlorobenzene solvent

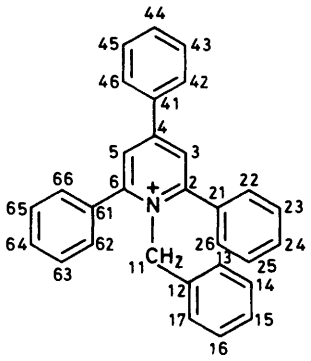

(**1**) BF_4^-

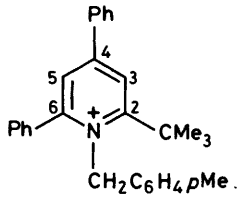

(**2**) BF_4^-

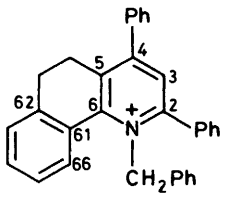

(**3**) $CF_3SO_3^-$

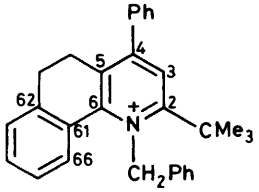

(**4**) BF_4^-

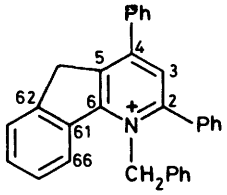

(**5**) BF_4^-

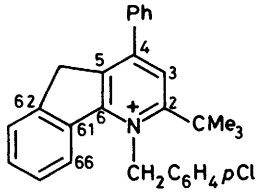

(**6**) BF_4^-

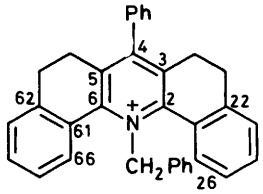

(**7**) ClO_4^-

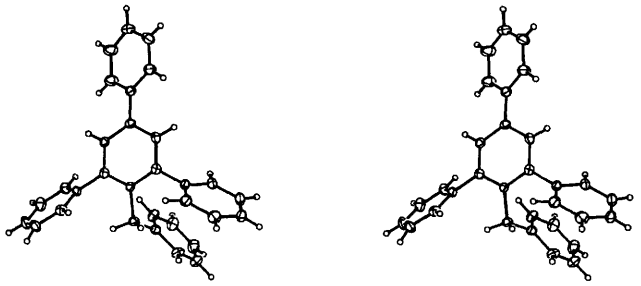

Figure 1. A stereoscopic projection of cation (**1**) (form **A**) from the crystal structure determination. In this and all other stereoscopic projections, the C and N atoms are depicted as the thermal ellipsoids for the 50% probability levels. Hydrogen atoms are depicted with arbitrarily small isotropic temperature factors

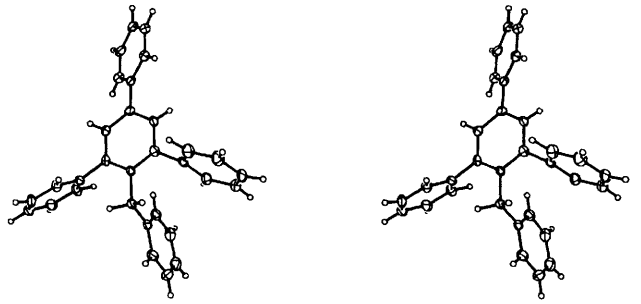

Figure 2. A stereoscopic projection of cation (**1**) (form **B**) from the crystal structure determination

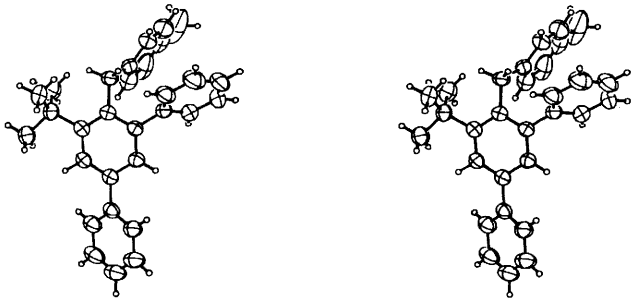

Figure 3. A stereoscopic projection of cation (**2**) from the crystal structure determination

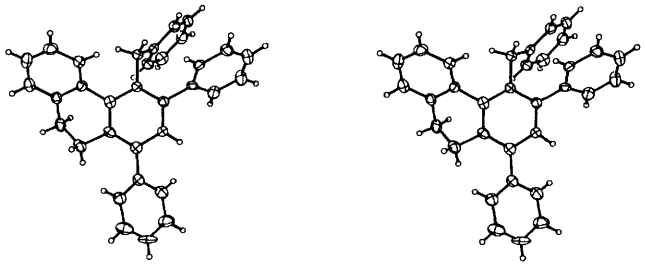

Figure 4. A stereoscopic projection of cation (**3**) from the crystal structure determination

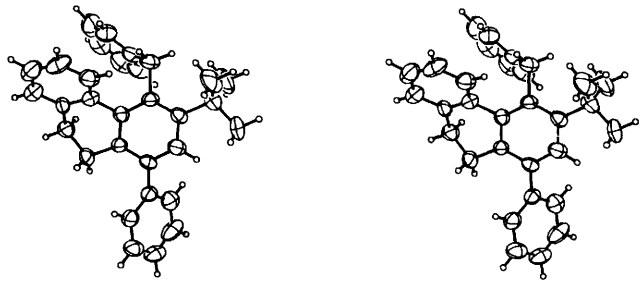

Figure 5. A stereoscopic projection of cation (**4**) from the crystal structure determination

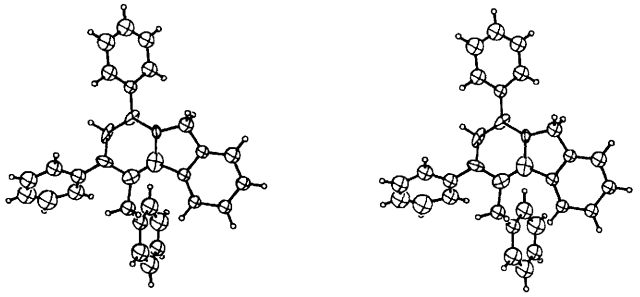

Figure 6. A stereoscopic projecton of cation (**5**) from the crystal structure determination

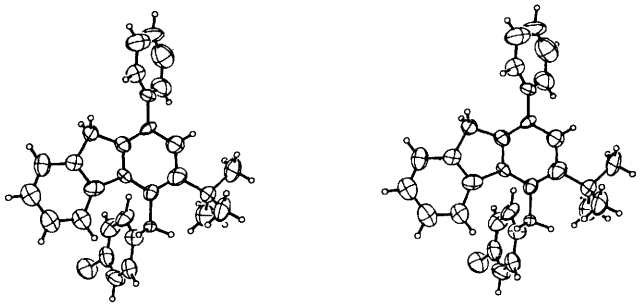

Figure 7. A stereoscopic projection of cation (**6**) from the crystal structure determination

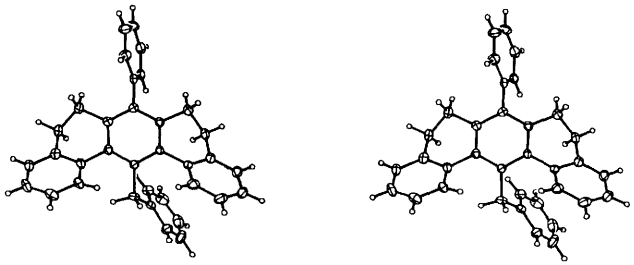

Figure 8. A stereoscopic projection of cation (**7**) from the crystal structure determination

were in the approximate ratio of 1:60:900. This was explained by the ease of twisting out of plane of the 2- and 6-phenyl groups in compound (**1**) which was largely prevented for one of the phenyl groups in (**3**) and for both the phenyl groups in (**7**). The effect of preventing twisting by annulation of a five-membered rather than a six-membered adjacent ring, as in compound (**5**), was very much less. Moreover, effects were not additive, thus t-butyl group substitution for phenyl in going from (**1**) to (**2**) reduced the rate whereas a similar change in going from (**3**) to (**4**) increased the rate.[3,4]

In view of the importance of reactions of this type from a preparative point of view,[5] we undertook an investigation of the *X*-ray crystal structures of compounds (**1**)—(**7**) in an attempt to

Table 1.[a] Crystal data and details of the structure analysis for compounds (1)—(7)

Formula	Compound (1) $C_{30}H_{24}BF_4N$	Compound (2) $C_{29}H_{30}BF_4N$	Compound (3) $C_{33}H_{26}F_3NO_3S$	Compound (4) $C_{30}H_{30}BF_4N$	Compound (5) $C_{31}H_{24}BF_4N$	Compound (6) $C_{29}H_{27}BClF_4N$	Compound (7) $C_{33}H_{28}ClNO_4$
M	485.33	479.37	577.66	491.08	497.32	511.80	538.04
Crystal system	Monoclinic	Monoclinic	Orthorhombic	Monoclinic	Monoclinic	Monoclinic	Monoclinic
T/K	*ca.* 130	298	*ca.* 130	298	298	298	*ca.* 130
a/Å	11.261(2)	45.41(1)	10.573(1)	11.386(2)	10.703(3)	10.827(4)	14.942(2)
b/Å	13.479(1)	8.378(2)	11.612(1)	16.771(3)	12.339(5)	13.467(4)	11.899(1)
c/Å	17.740(2)	14.223(3)	22.758(1)	13.839(1)	20.86(3)	17.940(3)	15.798(2)
β (°)	113.48(1)	108.08(2)	90	100.17(1)	114.64(2)	102.87(2)	109.87(1)
V/Å^3	2 470(1)	5 144(3)	2 794(1)	2 601(1)	2 503(1)	2 550(1)	2 642(1)
Space group	*Pc*	*C*2/*c*	$P2_12_12_1$	*Cc*	$P2_1/c$	$P2_1/n$	*P*2/*c*
Z	4	8	4	4	4	4	4
D_c/g cm^{-3}	1.31	1.238	1.36	1.254	1.282	1.341	1.38
D_m/g cm^{-3}	*b*	1.253	*b*	1.291	*b*	*b*	*b*
Radiation	Mo-K_α	Cu-K_α	Mo-K_α	Cu-K_α	Mo-K_α	Mo-K_α	Mo-K_α
λ/cm^{-1}	0.91	7.27	1.63	7.32	1.05	2.05	1.83
Crystal dimensions (mm)	(0.2 × 0.3 × 0.5)	(0.40 × 0.35 × 0.20)	(0.5 × 0.2 × 0.1)	(0.30 × 0.25 × 0.20)	(1.0 × 0.20 × 0.10)	(1.1 × 0.20 × 0.05)	(0.4 × 0.4 × 0.1)
Scan mode	ω	2θ/θ	2θ/θ	2θ/θ	2θ/θ	2θ/θ	ω
Scan rate (° min^{-1})	3—24	1.2—29.3	2—29.3	1.2—29.3	1.2—29.3	1.2—29.3	2—29.3
$2\theta_{max.}$ (°)	70	110	50	110	45	56	50
Total unique reflections	10 879	3 245	2 793	1 865	3 289	6 171	4 661
No. reflections used	9 519	2 053	2 793	1 415	865	1 688	4 661
No. variables refined	841	217	474	280	160	301	474
Coefficients of weighting function w[c]	*d*	24, 0, 1 0.003	0, 1, 0 0.0003	20.2, 0, 1 0.004	11, 0, 1 0.016	11, 0, 1 0.015	0, 1, 0 0.0008
Final R	0.094	0.056	0.073	0.065	0.094	0.104	0.106
Final R_w	0.078	0.074	0.045	0.088	0.118	0.133	0.068
Average e.s.d. for a C–C bond length (Å)	0.005	0.007	0.006	0.01	0.02	0.02	0.005

[a] E.s.d.s are given in parentheses. [b] Density not measured. [c] $1/w = a + b\,\sigma_{F_o} + cF + dF^2$. [d] $w \doteq (1 - e^{-10\sin^2\theta/\lambda^2})/(\sigma_{F_o} + 0.0007F^2)$.

Table 2. Relevant structural parameters of the pyridinium cations (**1**)—(**7**): $^{+}N-CH_2$ bond length and torsional angles of pyridinium ring with CH_2–aryl(^{+}N–C bond) and with α-phenyl ring (C–C bond). Relevant S_N2 reactivity data for the pyridinium cations (**1**)—(**7**): log k_2 for the reaction with piperidine in chlorobenzene at 100 °C

		Torsional angles (absolute values) (°) of pyridinium ring with CH_2–aryl bond				
Cation	$N^{+}-CH_2$ (Å) N(1)–C(11)	C(2)–N(1)–C(11)–C(12) θ(a)	C(6)–N(1)–C(11)–C(12) θ(b)	Sum θ(a) + θ(b)	Difference of sum from 180	log k_2[a]
(**1A**)	1.502(4)	103.8(4)	63.8(4)	167.6	12.4	−2.306[b]
(**1B**)	1.491(5)	91.0(4)	88.4(4)	179.4	0.6	
(**2**)	1.500(4)	110.9(4)	65.9(4)	176.8	3.2	−2.971[c,d]
(**3**)	1.509(5)	117.9(4)	50.5(4)	168.4	11.6	−0.465[d,e]
(**4**)	1.54(1)	114.3(9)	49.9(1)	164.2	15.8	−0.216[d,e]
(**5**)	1.47(2)	109(1)	80(2)	189	9	−0.975[e]
(**6**)	1.46(1)	97(1)	75(1)	172	8	*f*
(**7**)	1.512(4)	118.5(3)	45.0(3)	163.5	16.5	0.648[d,e]

[a] Logarithms of second-order rate constants for the reactions with piperidine in chlorobenzene at 100 °C. [b] From ref. 6. [c] Data for the *N*-benzyl cation. [d] Extrapolated at 100 °C from variable-temperature rate data. [e] From ref. 4. [f] Second-order rate constants could not be determined due to curvature of pseudo-first-order plots; *cf.* ref. 7.

Table 3. Relevant structural parameters of the pyridinium cations (**1**)—(**7**): torsional angles of pyridinium ring with α-phenyl groups (absolute values)

Cation	N(1)–C(6)–C(61)–C(62) θ(c)	N(1)–C(6)–C(61)–C(66) θ(d)	C(5)–C(6)–C(61)–C(62) θ(e)	C(5)–C(6)–C(61)–C(66) θ(f)	180° − [θ(c) + (d)]	180° − [θ(e) + θ(f)]	180° − [θ(c) + θ(e)]	180° − [θ(d) + θ(f)]	0.25 [360° − θ(c) + θ(d) + θ(e) − θ(f)]
(**1A**)	117.9(3)[a]	62.1(5)	58.9(5)	121.1(4)	0.0	0.0	3.2	3.2	60.5
	127.6(3)[b]	54.5(4)	50.8(4)	127.1(3)	2.0	2.1	1.7	1.6	52.7
(**1B**)	109.3(3)[a]	80.1(4)	72.4(4)	98.2(3)	9.4	9.4	1.7	1.7	76.3
	108.3(4)[b]	79.1(4)	71.9(4)	100.8(4)	7.4	7.3	0.2	0.1	75.5
(**2**)	120.0(4)	67.0(5)	59.9(5)	113.1(5)	7.0	7.0	0.1	0.1	63.5
(**3**)	151.0(4)[a]	37.1(6)	30.3(5)	141.6(4)	8.1	8.1	1.3	1.3	33.7
	130.5(4)[b]	53.9(5)	49.3(5)	126.4(4)	4.4	4.3	0.2	0.3	51.6
(**4**)	148.8(9)	36.1(1.3)	32.9(1.2)	142.2(9)	4.9	4.9	1.7	1.7	34.5
(**5**)	180(1)[a]	1(2)	3(1)	176(1)	1	1	3	3	2
	63(2)[c]	129(1)	111(1)	57(2)	12	12	6	6	60
(**6**)	179(1)	0(2)	2(1)	179(1)	1	1	1	1	1
(**7**)	144.3(3)[c]	39.2(4)	32.2(4)	144.2(3)	3.5	3.6	3.5	3.6	35.7
	151.8(3)[b]	34.1(4)	29.1(4)	145(3)	5.9	5.9	0.9	0.9	31.6

[a] Angles as defined at top of columns. [b] Angles as defined at top of columns, with consideration of the chemical equivalence of C(6) with C(2), C(61) with C(21), C(66) with C(26), C(5) with C(3), and C(62) with C(22). [c] Angles as defined at top of columns, but changing C(6) into C(2), C(61) into C(21), C(66) into C(22), C(5) into C(3), and C(62) into C(26).

Table 4. Relevant structural parameters of the pyridinium cations (**1**)—(**7**): closest non-bonded distances (Å) between CH_2 or '*ortho*' phenyl carbons and the adjacent groups

	Shortest distances C(11)–C(21) or C(11)–C(61)			Shortest distances C(11)–C(23) or C(11)–C(26) or C(11)–C(22), or C(11)–C(66)			Shortest distances C(13) or (17) to C(22), C(26), C(62), or C(66)		
Cation	free phenyl	fixed phenyl	t-butyl	free phenyl	fixed phenyl	t-butyl	free phenyl	fixed phenyl	t-butyl
(**1A**)	2.919(5)[a]			3.149(4)			3.766(5)[e]		
	2.829(4)[a]			3.132(5)			3.504(5)[f]		
(**1B**)	2.904(5)[b]			3.386(6)			4.080(6)[g]		
	2.899(5)[b]			3.395(5)			3.494(5)[h]		
(**2**)	2.799(5)		3.011(7)	3.136(6)		3.158(7)	3.713(6)[i]		3.527(6)
(**3**)	2.863(6)	2.947(6)		3.084(6)	3.012(6)		3.371(6)	3.590(6)[j]	
(**4**)		2.90(1)	3.05(0)		3.03(02)	3.10(2)[d]		3.50(2)	4.03(2)
(**5**)	2.86(2)	3.05(2)		3.20(2)	3.15(2)		3.66(3)	3.60(2)	
(**6**)		3.01(1)	2.94(1)		3.12(1)	3.08(1)		3.81(2)	3.57(2)
(**7**)		2.936(5)[c]			3.020(6)			3.459(5)[g]	
		2.917(5)[c]			3.038(5)			3.775(5)[e]	

[a–c] Exchange possible. [d] C(23) is involved. [e] Value is for C(17)–C(62). [f] Value is for C(13)–C(62). [g] Value is for C(13)–C(66). [h] Value is for C(17)–C(66). [i] Value is for C(13)–C(26). [j] Value is for C(13)–C(22).

obtain structure information useful for further characterization of the steric properties in the ground states and to help rationalize the observed rate differences.

Elucidation of the Crystal Structures.—Crystal data are collected in Table 1 and molecular structures are displayed as stereoscopic projections in Figures 1—8.

In Tables 2—7 we present structural parameters which we believe are relevant to the discussion.

Benzyl Group–Pyridine N–C *Bond Distances* (*Table* 2).—Significant variation (Table 2) is found in the length of the exocyclic C–N bond between the *N*-benzyl substituent and the pyridinium N atom. In previous work on unstrained com-

Table 5. Relevant structural parameters of the pyridinium cations (**1**)—(**7**): displacement of the methylene carbon (Å) and angles between selected planes (°)

	Displacement of CH_2 carbon			Angles between planes determined by C(12)–C(13)–C(17) and		
	from the plane of the pyridinium ring		from the plane N(1)–C(2)–C(6)			
Cation	distance	angle	distance	N(1)–C(2)–C(6)	C(21)–C(22)–C(23)[a] or C(26)	C(61)–C(62)–C(66)
(**1A**)	0.345	13.2	0.280	81.2	74.2[c]	26.6
(**1B**)	0.048	2.1	0.001	89.2	76.8[c]	62.9
(**2**)	0.16	6.1	0.7	86.0	51.4[b]	35.9
(**3**)	0.444	17.1	0.270	77.7	31.9[c]	56.9
(**4**)	0.69	23.7	0.38	72.5	70.9[b]	38.5
(**5**)	0.16	6.2	0.20	79.5	71.2[c]	82.3
(**6**)	0.25	9.8	0.17	80.7	23.0[b]	81.7
(**7**)	0.677	26.6	0.385	68.8	57.6[c]	41.7

[a] For the t-butyl groups we considered the plane determined by the carbon atoms closest to the methylene carbon, for instance C(21), C(22), and C(23). [b] C(23) is involved. [c] C(26) is involved.

Table 6. Inclinations (°) of the N(1)–C(11)–C(12) plane to the C(12)–C(13)–C(17) plane and distances (Å) of the nucleophile, placed at 2 Å from C(11), from the closest carbons of the 2,6-pyridine substituents in cations (**1**)—(**7**)

	Angle between N(1)–C(11)–C(12) and	Distances (Å) of the nucleophile from	
Cation	C(12)–C(13)–C(17) planes	C(26), C(22), or C(23)	C(66)
(**1A**)	42.6	4.12[a]	4.08
(**1B**)	8.2	4.40[a]	4.40
(**2**)	38.6	4.07[b]	4.04
(**3**)	49.4	4.05	3.99
(**4**)	52.1	4.20[c]	4.05
(**5**)	4.3	4.11[b]	3.99
(**6**)	4.8	3.91[b]	3.85
(**7**)	40.7	4.02	4.03

[a] C(26) is involved. [b] C(22) is involved. [c] C(23) is involved.

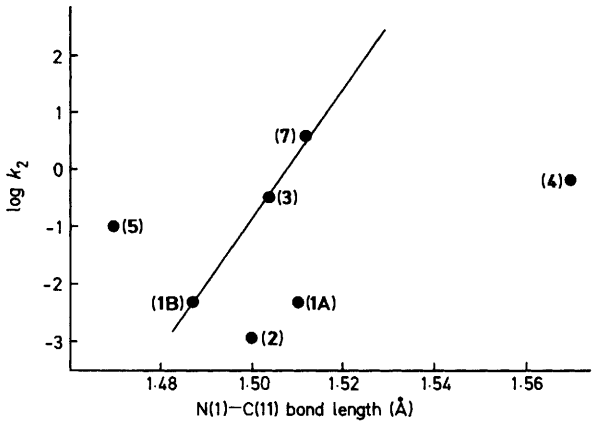

Figure 9. Plot of the logarithms of second-order rate constants for cations (**1**)—(**5**) and (**7**) with piperidine in chlorobenzene at 100 °C *versus* the N^+–CH_2 bond length (Å)

pounds such as 1-(2,6-dichlorobenzyl)-2-ethoxypyridinium fluoroborate[8] and 1-benzyl-2-[(hydroxyimino)methyl]pyridinium bromide or methanesulphonate,[9] this N–C distance was found to be in the range 1.484—1.499 Å. We find quite short bonds (1.46—1.47 Å) for the compounds containing annulated five-membered rings (**5**) and (**6**) and a very long bond (1.54 Å) for compound (**4**) which possesses both a fused six-ring *and* an α-t-butyl group. All the other compounds show bonds in the range 1.49—1.51 Å.

In Figure 9 the logarithms of second-order rate constants for the reactions of cations (**1**)—(**5**) and (**7**) with piperidine in chlorobenzene at 100 °C are plotted against the N–CH_2 bond length (Table 2). This plot shows a good correlation for the *N*-benzyl monocyclic, tricyclic, and pentacyclic derivatives (**1**), (**3**), and (**7**), with significant increase in rate on increasing the N–CH_2 bond length. However, increasing this bond distance within the tricyclic series [compounds (**3**)—(**5**)] causes little variation in rate, indicating that the constraint of one or both *ortho* phenyls to almost planarity with the pyridinium ring in the tricyclic and pentacyclic derivatives is the main structural feature of the leaving group which influences the rates. Of the two possible crystal environments in which (**1**) has been observed, only (**1B**) fits this scheme.

Torsional Angles about the N^+–CH_2 *Bond.*—These torsional angles θ(a) and θ(b) are defined and given in Table 2, together with their sum. For a planar pyridinium N atom, the sum should be 180°, consequently the deviation from this value provides a measure of the distortion of the N–C(1) bond out of the plane defined by atoms N(1), C(2), and C(6). The largest deviations are found for (**4**) and (**7**). Deviations for (**5**) and (**6**) are moderate. Remarkably, there is a large difference between the two crystallographically distinct molecules of (**1**):(**1A**) shows a rather large deviation, (**1B**) hardly any.

Torsional Angles about the C–C *Bonds connecting the* 2- *and* 6-*Aryl Groups to the Pyridinium Ring.*—These angles are defined as shown in Table 3. The deviations from 180° of the sums [θ (c) + θ(d)] and [θ(e) + θ(f)] provide a measure of the distortion of the α-phenyl rings from planarity. The phenyl groups of the fused five-membered rings of compounds (**5**) and (**6**) show almost no such distortion (*ca.* 1°). The phenyl groups in the fused six-membered rings of compounds (**3**), (**4**), and (**7**) show somewhat more distortion from planarity (3—6°). Such distortion torsional angle varies most widely for the non-fused phenyl groups of (**1A**), (**1B**), (**2**), (**3**), and (**5**) (from 0—12°).

The deviations from 180° of the sums [θ(c) + θ(e)] and [θ(d) + θ(f)] provide measures of the distortion of the pyridinium ring from its own planarity. For the supposedly symmetrical compounds (**1**) and (**7**), clearly the distortion of the pyridinium ring is greater on one side than the other. The same applies to the other two compounds (**3**) and (**5**), which contain two α-phenyl rings. It is difficult to discern any pattern for these distortions.

Table 7. Closest non-bonded distances (Å) between CH_2 and the adjacent groups for cations (**1**)—(**7**),[a] calculated assuming the N(1)–C(11) bond distances as 1.85 Å

	Shortest distance C(11)–C(21) or C(11)–C(61)						Shortest distance C(11)–C(26) or C(11)–C(62) or C(11)–C(22) or C(11)–C(66)						Shortest distance C(13) or C(17) to C(22) or C(26) or C(62) to C(66)					
	free		fixed				free		fixed				free		fixed			
Cation	phenyl	*D*	phenyl	*D*	Bu^t	*D*	phenyl	*D*	phenyl	*D*	Bu^t	*D*	phenyl	*D*	phenyl	*D*	Bu^t	*D*
(**1A**)	3.115	0.196					3.251	0.102				3.893[b]	0.127					
	3.014	0.185					3.230	0.098				3.797[c]	0.293					
(**1B**)	3.101	0.197					3.506	0.120				4.347[d]	0.267					
	3.096	0.197					3.513	0.118				3.594[e]	0.100					
(**2**)	2.98	0.181			3.21	0.199	3.220	0.084			3.25	0.092	3.93[b]	0.217			3.61	0.08
(**3**)	3.047	0.184	3.142	0.195			3.181	0.097	3.110	0.098			3.614	0.243	5.058	0.070[f]		
(**4**)			3.07	0.17	3.23	0.18			3.13	0.10	3.21[g]	0.11			3.70	0.20	4.10	0.07
(**5**)	3.06	0.200	3.27	0.22			3.30	0.10	3.23	0.08			3.71	0.05	3.64	0.04		
(**6**)			3.23	0.22	3.15	0.21			3.17	0.05	3.16	0.08			3.84	0.03	3.62	0.05
(**7**)			3.129[h]	0.193					3.121[i]	0.101					3.703[d]	0.244		
			3.108[j]	0.191					3.139[k]	0.101					3.946[b]	0.171		

[a] Differences from the corresponding values in Table 4 are indicated as *D*. [b] Value for C(17)–C(62). [c] Value for C(13)–C(62). [d] Value for C(13)–C(66). [e] Value for C(17)–C(66). [f] Value for C(13)–C(22). [g] C(23) is involved. [h] Value for C(11)–C(21). [i] Value for C(11)–C(26). [j] Value for C(11)–C(61). [k] Value for C(11)–C(66).

The average values of 0.25 [360 − θ(c) + θ(d) + θ(e) − θ(f)] give a measure of the twisting of the average plane of the *C*-phenyl group out of the average plane of the pyridinium ring. It is striking that the phenyl groups in fused five-membered rings [(**5**), (**6**)] are almost coplanar with the pyridinium ring (1, 2°). Phenyl groups in the fused six-membered rings are twisted out of the pyridinium ring plane by 32—36° [in compounds (**3**), (**4**), and (**7**)] whereas twisting in the 'free' phenyl groups is considerably greater at 52—76°.

The value of 360 − [θ(c) + θ(d) + θ(e) + θ(f)] should be zero [because θ(c) + θ(d) = θ(e) + θ(f)]: this is found to be so for all compounds and this provides a check of the consistency of the calculations.

Non-bonded Distance between CH_2 and 2- *and* 6-*Substituents* (*Table* 4).—The distances C(11)–C(21) and C(11)–C(61) are all in the interval 2.80—3.05 Å. This distance increases with the distortion of the N(1)–C(11) bond and the C(2)–C(21) bond away from each other (which could occur by bond angle distortion). Understandably, these distances are smallest (2.80—2.92 Å) when they involve a free phenyl which can rotate out of the plane and thus relieve steric congestion. They increase for the fixed phenyl groups, and for t-butyl to 2.90—3.05 Å.

The distances C(11)–C(22) *etc.* are all in the interval 3.01—3.40 Å. Within this range the fixed phenyl groups usually show as expected shorter distances (all below 3.16 Å) than the free phenyls (all except one above 3.13 Å). Of the fixed phenyls those fixed by a six-membered ring tend to show shorter distances than those fixed by a five-membered ring.

Distances C(13)–C(22) *etc.* vary over the range 3.37—4.99 Å, but no regular pattern can be discerned.

Out-of-plane Displacement of the Benzyl CH_2 *Group.*—Table 5 gives displacements of the CH_2 group (a) from the average plane of the pyridinium ring (both as a distance and as an angle) and (b) from the plane N(1), C(2), C(6). The angles of displacement of CH_2 from the pyridinium ring plane (α) correlate with the nucleophilic displacement rates, largest for (**4**) and (**7**) less for (**3**), still less for (**6**), and least for (**2**) and (**5**). Figure 10 records the plot of the S_N2 rates (Table 6) *versus* the angle α, *i.e.* the displacement of the methylene carbon from the average plane of the pyridinium ring (Table 5). In analogy to Figure 9, a correlation with a significant rate enhancement on increasing the angle α is found for the *N*-benzyl series (**1**), (**3**), and (**7**), while rates vary much less within the tricyclic sequence. Accordingly, very different reactivities can be observed for compounds with very similar α values: thus the tricyclic derivative (**5**) is more than two orders of magnitude faster than the monocyclic (**2**) and similarly the pentacyclic (**7**) is much more reactive than the tricyclic (**4**).

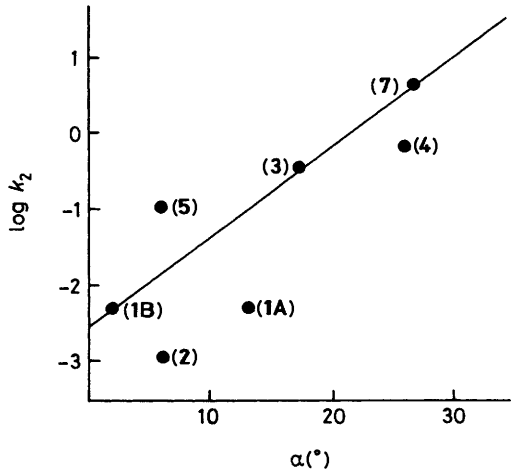

Figure 10. Plot of the logarithms of second-order rate constants for cations (**1**)—(**5**) and (**7**) with piperidine in chlorobenzene at 100 °C *versus* the displacement of the CH_2 carbon from the plane of the pyridinium ring (angle α)

Again the two crystallographic forms of (**1**) show rather different values of α, one very small and one somewhat larger, and (**1B**) is that which fits this plot better.

Orientation of the Benzyl Ring Plane.—Table 5 also gives the angles showing the orientation of the plane of the benzyl ring to those of the pyridinium and α-phenyl rings.

Of greatest significance is the angle between the planes of the benzyl ring and the pyridinium ring *i.e.* C(12), C(13), C(17) *versus* N(1), C(2), C(6) in Table 5. This parameter shows an excellent correlation with the rate for all the compounds (Figure 11). Given that the linking CH_2-carbon atom is tetrahedral, it can only vary between *ca.* 72 (180 − 108) and 90° and

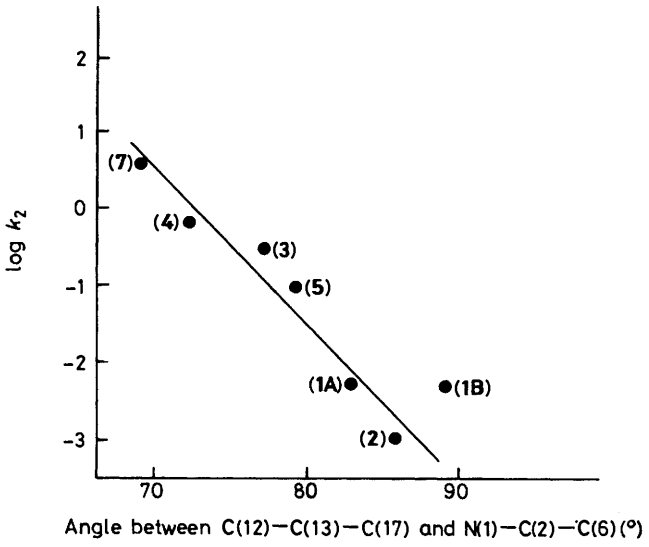

Figure 11. Plot of the logarithms of second-order rate constants for cations (**1**)—(**5**) and (**7**) with piperidine in chlorobenzene at 100 °C *versus* the angles between planes determined by C(12)–C(13)–C(17) and N(1)–C(12)–C(6)

does in fact vary over almost this very range. This parameter is significant in that it reflects the possibility of overlap of the incoming nucleophile with the π-electrons of the phenyl ring of the benzyl group which will be at a minimum when this angle is 90° and will increase as the angle decreases towards 72°.

The angles of the *N*-benzyl ring plane to the phenyl ring plane vary widely, but it is difficult to discern a regular pattern.

Ease of Nucleophile Access.—In a bimolecular displacement reaction at a benzylic carbon atom, the favoured approach path would be (a) perpendicular to the C(12), C(13), C(17) plane so that maximum overlap with the π-cloud is possible, and simultaneously (b) along the lines of the N(1)–C(11) bond, so that entering group, C atom, and leaving group are collinear. Table 6 shows the inclination of N(1)–C(11)–C(12) plane to the C(12)–C(13)–C(17) plane. The nearer this angle is to 90°, the easier should be nucleophilic displacement. The compounds fall clearly into two groups, very small angles for (**5**) and (**6**) [and one of the forms of (**1**)] and angles near 45° for the other compounds. This may explain in part the low displacement rates found for compounds (**5**) and (**6**) with fused five-membered rings.

For further data in Table 6, we have placed the nucleophile on the N(1)–C(11) lines at 2 Å from C(11) in the opposite direction to N(1). We record the distances of 'Nu' from C(26) and C(66): these distances are remarkedly similar and do not explain the rate variations found.

Tendency towards Unimolecular Dissociation.—In Table 7 we have recorded the increase in the non-bonded interaction distances of Table 4 when the N(1)–C(11) bond distance is increased to 1.85 Å in all the compounds, the other distances and angles being held constant.

The increases in the distance C(11)–C(21) and C(11)–C(26) appear to be almost constant throughout the series. However, for the distance C(13)–C(22) we find what seems to be significant variations: increases are small (<0.1) for Bu^t groups and for phenyls in a fused five-membered ring, but relatively larger (>0.2) for free phenyls or phenyls in a fused six-membered ring. The first group of compounds has a greater tendency to S_N1 dissociation, and the possibility that this may be related is being followed up by calculations.

Conclusions.—We believe that the foregoing discussion demonstrates a correlation between reaction rates and the molecular geometry. The strain existing in all these molecules can clearly be relieved in a number of different ways (bond lengthening, ring distortion, *e.g.* non-planarity, angle change) which are manifested to differing extents in different molecules. Hence, the kinetic rates do not correlate closely with most of the geometrical parameters, although an excellent correlation is found (Figure 11) with the geometrical feature which determines the overlap possible for the incoming nucleophile with the π-electron cloud of the benzyl group.

The considerable differences found in the geometry of the two crystallographically distinct triphenylpyridinium cations should, however, lend caution to such correlations with single geometrical parameters. It is also implicit in these considerations that the crystallographic form adopted by the cations is maintained in chlorobenzene solution. We are now making calculations of the conformations of these cations and the detailed geometrical parameters will be compared with calculated values.

Experimental

The preparation of compounds (**1**),[10] (**2**),[7] (**3**),[11] (**4**),[4] (**5**),[4] (**6**),[7] and (**7**)[11] has been reported. Suitable single crystals of (**2**), (**4**), (**5**), and (**6**) were obtained by slow evaporation at room temperature from ethanol, aqueous ethanol, acetone–ethanol, and acetonitrile, respectively. Crystals of compounds (**1**), (**3**), and (**7**) were each grown by vapour diffusion at 20 °C of light petroleum (b.p. 40—60 °C) into ethanol solutions.

X-*Ray Data Collection.*—Details are given in Table 1.

X-*Ray Structure Determination.*—Lattice parameter and intensity measurements were made with the following four-circle-diffractometers, a Syntex $P\bar{1}$ with low-temperature device LT-1 for compound (**1**), a Syntex $P2_1$ for compounds (**2**), (**4**), (**5**), and (**6**) and a Nicolet R3 with LT-1 for compounds (**3**) and (**7**), each equipped with graphite monochromator crystals. Crystal data and further characterization of the data sets are contained in Table 1.

The usual corrections, except for absorption, were applied to the intensities. Initial structural models were obtained by MULTAN[12] for compounds (**1**), (**2**), and (**4**)—(**6**) and SHELXTL[13] for (**3**) and (**7**) and were developed by difference Fourier and least-squares methods.* For (**1**), (**3**), and (**7**) the H atoms were located by difference Fourier syntheses and were refined with isotropic temperature factors; the remaining atoms were refined with anisotropic temperature factors. Hydrogen atoms for (**2**) and (**4**)—(**6**), calculated from standard geometries (C–H 1.00 Å), contributed to structure factor calculations with isotropic temperature factors equal to those of the atoms to which they were bonded but were not refined. No efforts were made to determine absolute configurations for structures with noncentrosymmetric space-groups, nor was any special effort made to correlate enantiomer selection throughout the series of compounds. The final refinements were carried out with full matrix for (**4**), with block-diagonal matrix for (**2**), (**5**), and (**6**), and a blocked cascade procedure with *ca.* 100 variables per block for (**1**), (**3**), and (**7**). In all cases $w(\Delta F)^2$ was minimized. The final difference Fourier maps showed no significant features.

Structures (**4**)—(**6**) present disorder in the tetrafluoroborate anion and all four room temperature structures are generally affected by large temperature factors. For the anions of the low-temperature structures, the largest mean-square deviation along the principal axis of a thermal ellipsoid is 0.171 Å^2.

* The *X*-Ray system[14] and finally SHELXTL[13] was used for structure (**1**), the CAOS package[15] for structures (**2**) and (**4**)—(**6**), and SHELXTL[13] for structures (**3**) and (**7**).

Acknowledgements

We thank the N.S.F. U.S.A.–Spain Committee for support which helped in the final preparation of this manuscript.

References

1 Part 24, A. R. Katritzky and B. Brycki, *J. Am. Chem. Soc.*, 1986, **108**, 7295.
2 For a review see A. R. Katritzky and G. Musumarra, *Chem. Soc. Rev.*, 1984, **13**, 47.
3 A. R. Katritzky, G. Musumarra, and K. Sakizadeh, *Tetrahedron Lett.*, 1980, **21**, 2701.
4 A. R. Katritzky, A. M. El-Mowafy, G. Musumarra, K. Sakizadeh, C. Sana-Ullah, S. M. M. El-Shafie, and S. S. Thind, *J. Org. Chem.*, 1981, **46**, 3823.
5 For reviews see (*a*) A. R. Katritzky, *Tetrahedron*, 1980, **36**, 679; (*b*) A. R. Katritzky and C. M. Marson, *Angew. Chem., Int. Edn. Engl.*, 1984, **23**, 420.
6 A. R. Katritzky, G. Musumarra, K. Sakizadeh, and M. Misic-Vukovic, *J. Org. Chem.*, 1981, **46**, 3820.
7 A. R. Katritzky, W. H. Basinski, Y. X. Ou, G. Musumarra, and R. C. Patel, *J. Chem. Soc., Perkin Trans. 2*, 1982, 1055.
8 G. L. Wheeler and H. L. Ammon, *Acta Crystallogr.*, 1974, **B30**, 680.
9 W. Van Havere, A. J. Lenstra, and H. J. Geise, *Acta Crystallogr.*, 1982, **B38**, 469.
10 A. R. Katritzky, U. Gruntz, D. H. Kenny, M. C. Rezende, and H. Sheikh, *J. Chem. Soc., Perkin Trans. 1*, 1979, 430.
11 A. R. Katritzky, A. M. El-Mowafy, L. Marzorati, R. C. Patel, and S. S. Thind, *J. Chem. Res.* (*S*), 1980, 310; (*M*), 1980, 4001.
12 P. Main, S. E. Hull, L. Lessinger, G. Germain, J. P. Declercq, and M. M. Woolfson, MULTAN 78, a System of Computer Programs for the Automatic Solution of Crystal Structure from *X*-Ray Diffraction Data, Universities of York and Louvain, 1978.
13 G. M. Sheldrick, SHELXTL, An Integrated System for Solving, Refining and Displaying Crystal Structures from Diffraction Data, University of Goettingen, version 2.5, 1980, and version 3.0, 1981.
14 The *X*-Ray System, Version of 1976, J. M. Stewart, Technical Report TR-446, Computer Science Center, University of Maryland.
15 S. Cerrini and R. Spagna, Abstracts 5th European Crystallographic Meeting, Oxford, 1977.

Received 24*th February* 1986; *Paper* 6/385